Cranial Vascular Anatomy and Its Variations

2

Petros Zampakis

Arterial Cranial Anatomy and Variations

The internal carotid arteries (ICAs) supply the so-called anterior cerebral circulation while the vertebral forming the basilar artery supply the posterior circulation. Those systems meet at the Circle of Willis (COW).

Anterior Circulation

The ICA consists of seven embryonic segments and this "embryonic" classification can explain the configuration and distribution of segmental agenesis and other anatomic variations [1].

ICA enters the cranial cavity through the carotid canal of petrous bone. For clinical purposes, the seven anatomical segments classification system by Bouthillier, is currently widely accepted -C1 cervical, C2 petrous, C3 lacerum, C4 cavernous, C5 clinoid, C6 ophthalmic and C7 communicating [2].

Two small but important branches arise from the cavernous ICA (C4). The tentorial and inferior hypophyseal artery may arise as a meningohypophyseal trunk. The inferolateral trunk supplies adjacent cranial nerves and anastomoses with the external carotid (ECA).

A very important anatomic landmark and a subject of great surgical attention, is the "transitional" or clinoid area of ICA. The vessel passing this area goes through the so-called distal dural ring and becomes intradural-subarachnoid. This transition is critical, because aneurysms past the aforementioned point are located in the subarachnoid space, and their rupture leads to subarachnoid hemorrhage. In the

P. Zampakis, MD, PhD, MSc
Department of Radiology, University Hospital of Patras, Rion, Greece 26500
e-mail: pzampakis@gmail.com

A. Agrawal, G. Britz (eds.), *Pediatric Vascular Neurosurgery*,
DOI 10.1007/978-3-319-43636-4_2

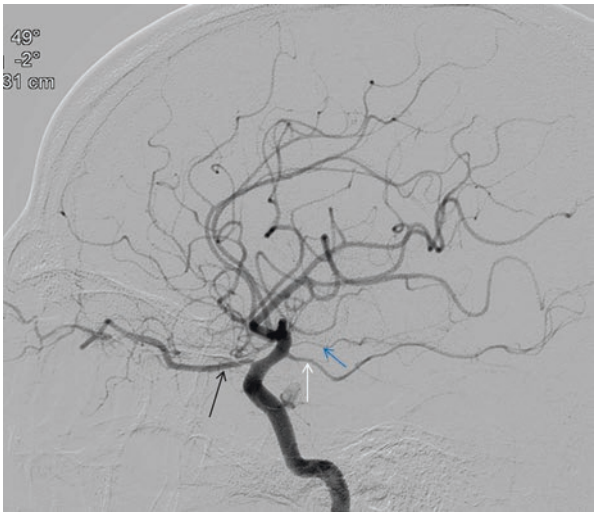

Fig. 2.1 Cerebral angiogram of the ICA (oblique view). *Black arrow* shows the ophthalmic artery (*OA*), the first major branch of ICA, which is the anatomic landmark of the distal dural ring. Anterior choroidal artery (*blue arrow*) and fetal type of posterior communicating artery (*white arrow*) are also seen

majority of people (~90 %) the ophthalmic artery which is the first major branch of ICA, is usually located distal to the distal dural ring (Fig. 2.1).

The C7 segment of ICA gives rise to two important branches, the posterior communicating artery (pCom) and the anterior choroidal artery. The former is part of the COW anastomotic network, varying in size and sometimes occurring as a fetal-type posterior communicating artery. The latter supplies the posterior limb of internal capsule, cerebral peduncle and optic tract, medial temporal lobe and choroid plexus (Fig. 2.1).

The main anatomic variations of ICA include course deviations [3] and segmental agenesis of the vessel, where each of these embryonic vessels represents the potential point of vascular reconstitution of flow into the distally preserved ICA. The aberrant course of ICA is such a configuration. In children, the diagnosis of course variations (especially the retropharyngeal course of ICA) must always be predicted, especially prior to adenotonsillectomy, in order to avoid catastrophic complications [4, 5]. Generally, knowledge of these variations is crucially important for neck surgery.

The terminal ICA is divided into the anterior (ACA) and middle cerebral arteries (MCA).

The ACA is divided into four segments: horizontal segment (A1), vertical segment (A2), genu segment (A3) and terminal portions (A4-A5) (Fig. 2.2a). The A1 segment is connected to the contralateral A1 segment by the anterior communicating artery (AcomA). The A1 segment gives rise to small perforating branches, the medial lenticulostriate arteries (LS). The recurrent artery of Heubner is the largest of the perforating branches, arising from the A1 or A2 segment (in 80 %).

The A2 segment gives rise to orbitofrontal artery and frontopolar artery, while A3 segment gives rise to pericallosal and callosomarginal arteries (Fig. 2.2b).

Surface branches supply the cortex and white matter of the inferior frontal lobe, the medial surface of the frontal and parietal lobes, as well as the anterior corpus

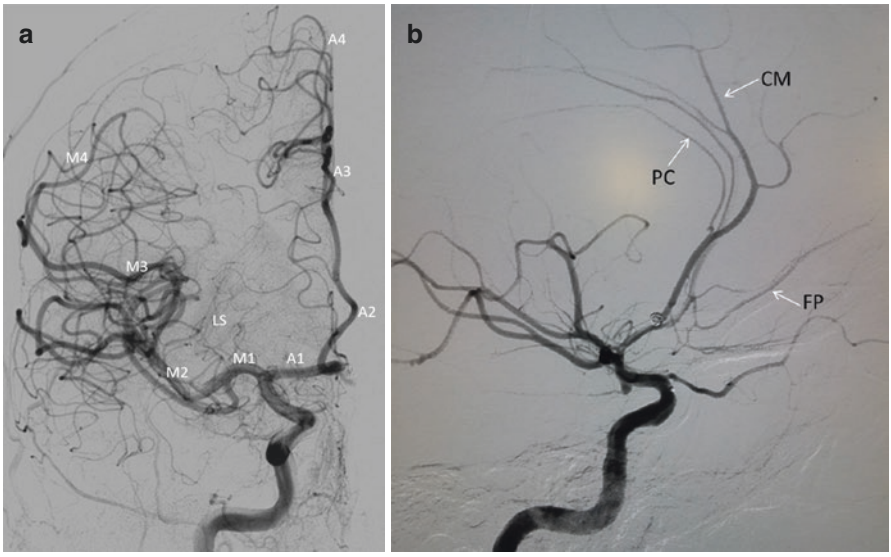

Fig. 2.2 (**a**) Cerebral angiogram of the R ICA (AP view). The segments of middle cerebral artery (MCA/M1-M4) and anterior cerebral artery (ACA/A1-A4) are annotated. *LS* lenticulostriate arteries. (**b**) Cerebral angiogram of the R ICA (lateral view). Branches of anterior cerebral artery are annotated. *CM* callosomarginal art, *PC* pericallosal art, *FP* frontopolar art

callosum. Penetrating branches supply the deeper cerebrum, diencephalon, the limbic structure, and head of caudate as well as the anterior limb of internal capsule.

Anatomic variations are very common in the first two segments of anterior cerebral artery, including hypoplasia, absence or fenestration of A1, variations of recurrent artery of Heubner (Accessory middle cerebral artery) and unpaired ACA configuration (including azygos artery and bihemispheric ACA) (Fig. 2.3a, b), as well as triplicated ACA.

The most common variant (~27 %) is the presence of hypoplastic A1 segment of ACA (Fig. 2.4), while aplasia of A1 is less common (Fig. 2.5a–c) [6].

Aplasia of A1 is an important variation in cases of Acom aneurysms, where the neurointerventionist must be aware that possible compromisation of the neck of the aneurysm (either endovascular or surgical), could lead to bilateral frontal lobe ischemic events. The same applies to the presence of an unpaired ACA (short or long segment) [7].

Although aplasia or hypoplasia of A1 is constantly seen in the vast majority of patients with Acom aneurysms, their role in the formation of aneurysms is unclear.

MCA, which is the phylogenetically youngest of all cerebral vessels, is divided into four anatomical segments: horizontal segment (M1), insular segment (M2), opercular segment (M3) and cortical branches (M4 segments) (Fig. 2.2a). The M1 segment gives off medial and lateral lenticulostriate arteries (perforating branches supplying basal ganglia and capsular regions), as well as anterior temporal artery for the anterior temporal lobe. Then, it divides as a bifurcation or trifurcation. Cortical branches supply the lateral surface of the cerebral hemispheres (Fig. 2.6).

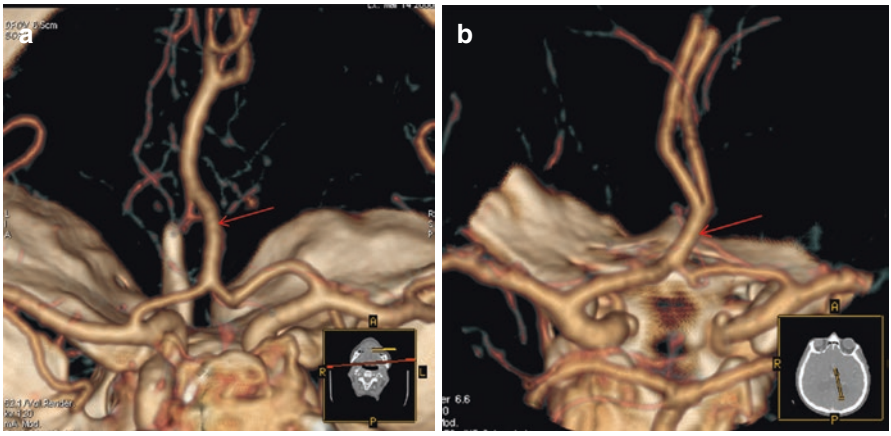

Fig. 2.3 (**a**) CTA (VRT 3D reconstructions) reveals the presence of an unpaired ACA (conventional type, long segment) (*red arrow*) (Reproduced from Zampakis et al. [6]) (**b**) CTA (VRT 3D reconstructions) shows an unpaired ACA (conventional type, short segment) (*red arrow*) (Reproduced from Zampakis et al. [6])

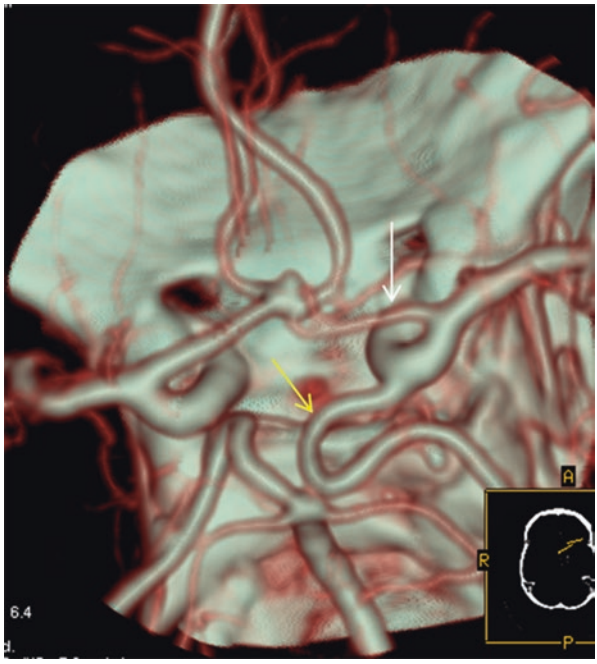

Fig. 2.4 CTA (VRT 3D reconstructions) shows a hypoplastic right sided A1 segment of anterior cerebral artery (*white arrow*), in a patient with an Acom aneurysm. Note the presence of a fetal Pcom on the same side (*yellow arrow*) (Reproduced from Zampakis et al. [6])

Relatively few MCA variants are present, the Accessory MCA (AccMCA) being the most important one. Other less clinically significant variants include early disposition of cortical branches (from M1 segment), duplication and fenestration of various segments [8].

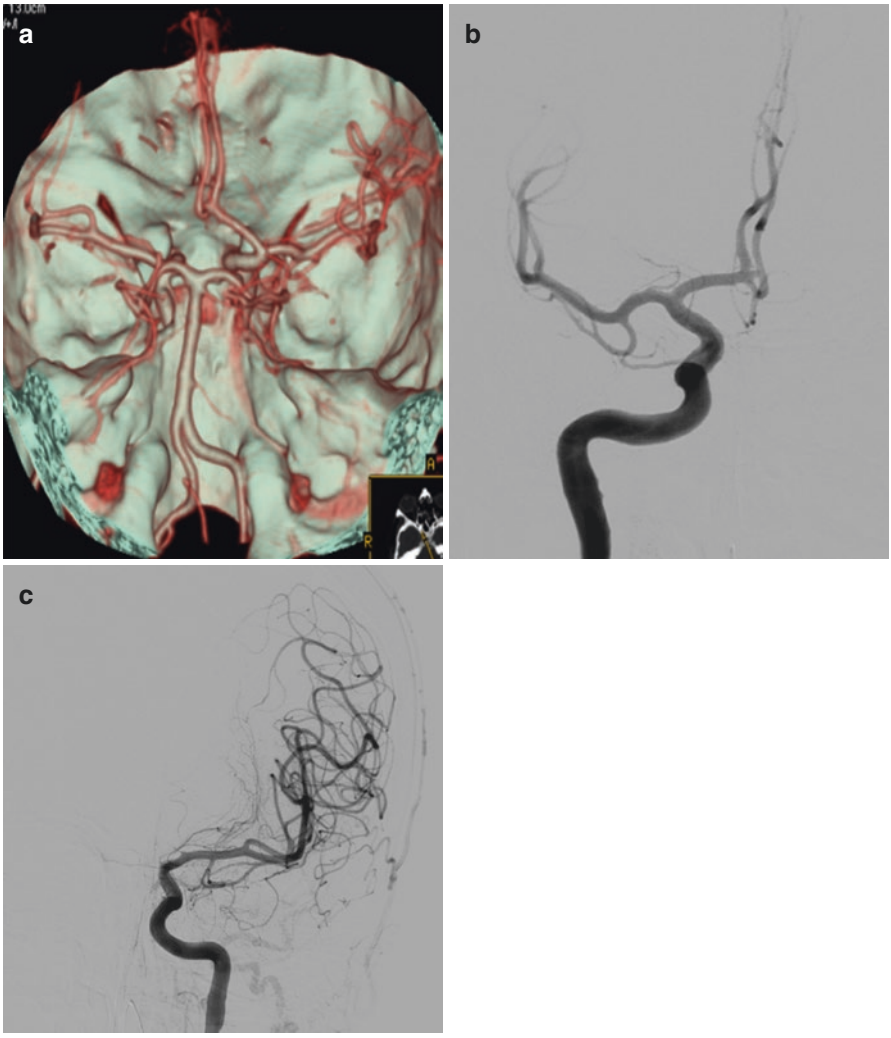

Fig. 2.5 (**a**) CTA (VRT 3D reconstructions) reveals aplasia of left A1 segment of anterior cerebral artery, in a patient with an Acom aneurysm (Reproduced from Zampakis et al. [6]). (**b**) Digital substraction angiography (AP view) of the right ICA, verifies the presence of a small Acom aneurysm. Both A2 segments are opacified, from this single injection (Reproduced from Zampakis et al. [6]). (**c**) Digital substraction angiography (AP view) of the left ICA. The left A1 segment is absent (Reproduced from Zampakis et al. [6])

The variations of the AccMCA express the phylogenetic origins of the MCA from a group of vessels with similar potentials in the early stages of evolution, including the recurrent artery of Heubner (RAH). Therefore, a distal ACA origin of the AccMCA corresponds to an enlarged RAH. This has been described by Manelfe

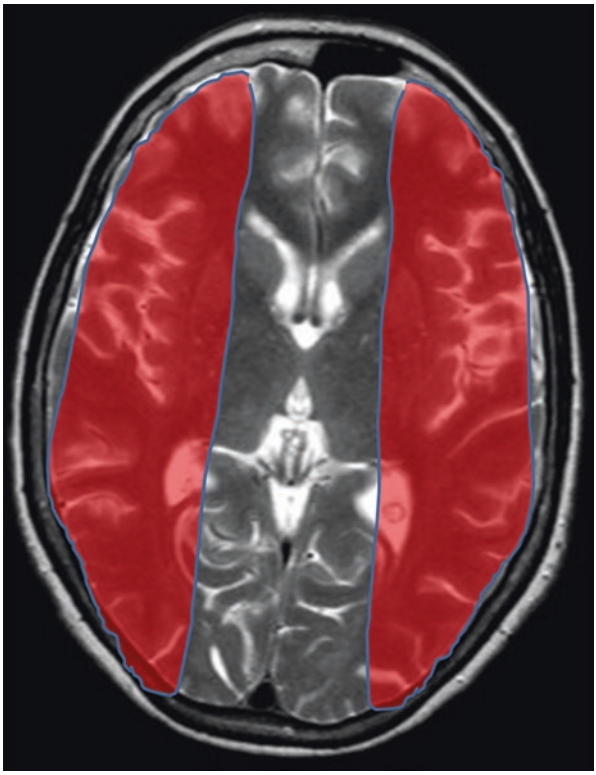

Fig. 2.6 Brain MRI. Axial T2 image at the level of lateral ventricles. *Red areas* indicate the vascular territory of cortical branches of MCA

in 1977 as type 3, where AccMCA is a Heubner artery with an extensive cortical supply, arising from the proximal part of A2 segment [9].

The most important clinical role of AccMCA is in cases of severe stenosis/occlusion of proximal carotid, where this vessel is actually a natural by-pass [10, 11] (Fig. 2.7a–e).

Posterior Circulation

The vertebral arteries (V4 segment) enter the cranial cavity, via foramen magnum. The vessel gives rise to the posterior inferior cerebellar artery (PICA) supplying the brainstem, inferior cerebellar hemisphere, vermis and the choroid plexus, before it forms basilar artery.

The latter runs superiorly on the anterior surface of the pons giving off anterior inferior cerebellar (AICA), superior cerebellar (SCA) and posterior cerebral arteries (PCAs) on both sides as well as perforating branches for brainstem (Fig. 2.8a, b).

The AICAs supply the anterior inferior part of cerebellum, as well as the internal auditory meatus nerves. Its cerebellar branches anastomose with those of the PICA. The SCAs arise right below the basilar tip and supply the superior part of the cerebellar hemispheres.

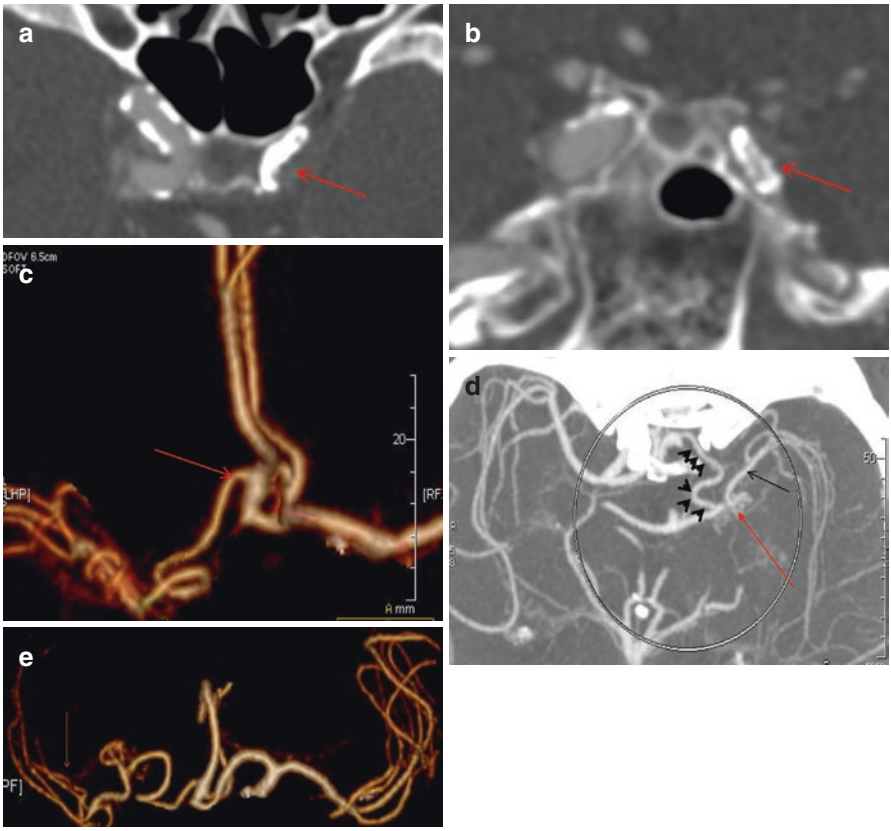

Fig. 2.7 (**a**) Axial CT image at the level of cavernous carotids shows occlusion of the left ICA (*red arrow*), due to atherosclerotic disease (Reproduced from Zampakis et al. [6]). (**b**) Coronal reconstruction at the level of cavernous carotids verifies the occlusion of the left ICA (*red arrow*), as well as the atherosclerotic disease (Reproduced from Zampakis et al. [6]). (**c**) CTA (VRT 3D reconstructions) shows the accessory MCA as a vessel coming from the A2 segment of ipsilateral anterior cerebral artery (*red arrow*) (Reproduced from Zampakis et al. [6]). (**d**) Axial MIP image shows the course of AccMCA (*black arrowheads*), the anastomotic network (Moya-Moya type) at the level of left mid M1 segment (*red arrow*), as well as the patent peripheral left MCA (*black arrow*) (Reproduced from Zampakis et al. [6]). (**e**) CTA (VRT 3D reconstructions) reveals the same configuration and patent peripheral MCA (*red arrow*) (Reproduced from Zampakis et al. [6])

The posterior cerebral arteries are the terminal branches of the basilar artery, each of which has four segments. These are the precommunicating (P1), ambient (P2) quadrigeminal (P3) and finally P4 segment which is the terminal segment including the occipital and inferior temporal branches (Fig. 2.9).

There is diversity in caliber of the P1 segment of the PCAs and pComs. One edge of this diversity is the so-called fetal origin of the posterior cerebral artery, where the P1 segments may be hypoplastic and even invisible on vertebral angiography. The posterior communicating arteries and P1 segments give off the thalamoperforating

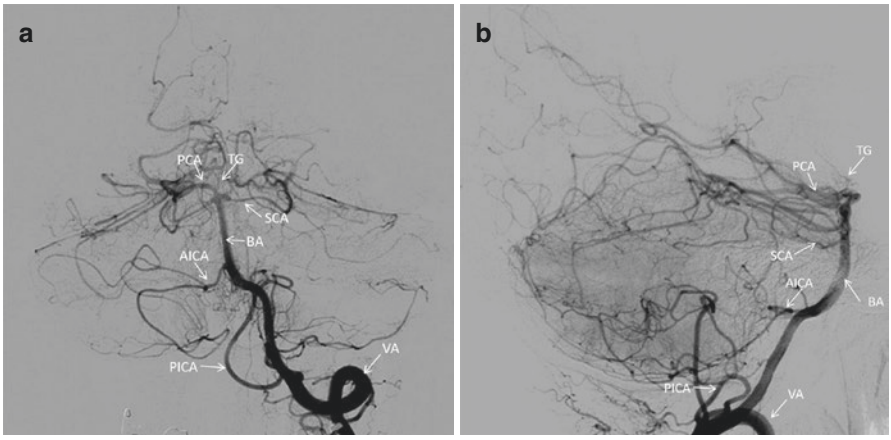

Fig. 2.8 (**a**) Selective angiogram of the L vertebral artery (AP view). Vertebral artery (*VA*), basilar artery (*BA*), posterior inferior cerebellar artery (*PICA*), anterior inferior cerebellar artery (*AICA*), superior cerebellar artery (*SCA*), posterior cerebral artery (*PCA*), thalamogeniculate (*TG*) perforating arteries. (**b**) Selective angiogram of the L vertebral artery (lateral view). Vertebral artery (*VA*), basilar artery (*BA*), posterior inferior cerebellar artery (*PICA*), anterior inferior cerebellar artery (*AICA*), superior cerebellar artery (*SCA*), posterior cerebral artery (*PCA*), thalamogeniculate (*TG*) perforating arteries

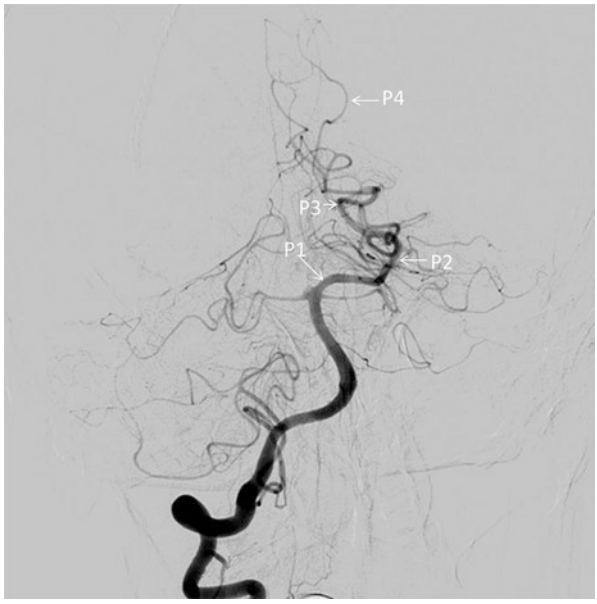

Fig. 2.9 Selective angiogram of the R vertebral artery (AP view). The segments of posterior cerebral artery (PCA/P1-P4) are annotated

arteries and thalamogeniculate arteries. Medial and lateral posterior choroidal arteries arise from the P2 segment and seem to be the main arterial feeders to Vein of Galen malformation or other arteriovenous malformations located in this area (Fig. 2.10a, b). Temporal branches (anterior, posterior, inferior), parieto-occipital

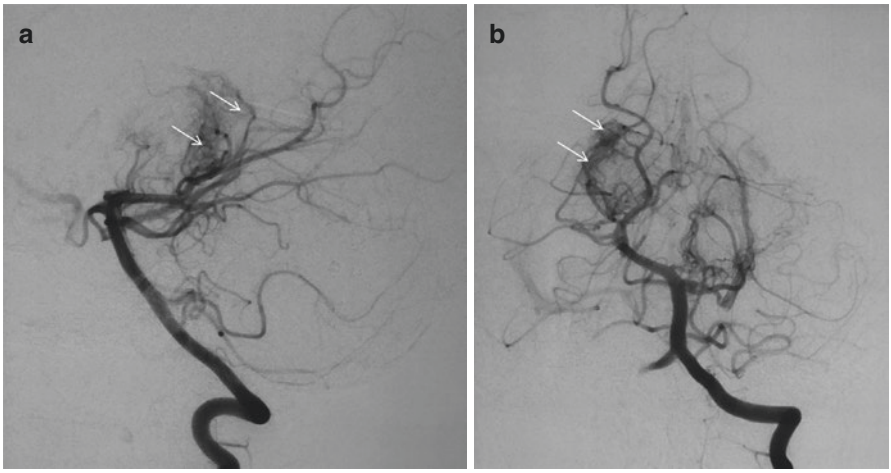

Fig. 2.10 (**a**) Selective angiogram of the L vertebral artery (Lateral view). Posterior choroidal arteries (*white arrows*) are the arterial feeders of a diffuse type arteriovenous malformation in a 7 year old girl. (**b**) Selective angiogram of the L vertebral artery (AP view). Posterior choroidal arteries (*white arrows*) are the arterial feeders of a diffuse type arteriovenous malformation in a 7 year old girl

artery and calcarine artery, are cortical branches supplying a large part of the inferior surface of the temporal lobe and the medial surface of the occipital lobe, including the visual cortex.

Most clinically important anatomic variations of posterior circulation system include "fetal" arrangement of PCA, other persistent carotid-basilar anastomosis and symmetric or asymmetric caudal fusion of the tip of basilar artery. Other variants include hypoplastic or aplastic V4 segment and fenestrations of basilar artery.

Persistent carotid-basilar anastomoses are actually developmental connections between the anterior (carotid) and posterior (vertebrobasilar) circulation that may persist into adult life.

By far the most common and clinically important persistent carotid-basilar anastomosis is the presence of fetal type of posterior communicating artery (Figs. 2.11 and 2.12) [6]. In this case, practically the PCA comes from the ICA.

Its knowledge plays an important role in patients with Pcom aneurysms, where this vessel comes out of the aneurysmal sac. If this variation occurs, the neurointerventionist should definitely protect the fetal pcom, in order to avoid occipital lobe infarct (Fig. 2.13a–d). Another important clinical significance is that carotid pathology may cause a "posterior circulation" stroke (Fig. 2.14a–c).

Other anastomoses include persistent hypoglossal artery (Fig. 2.15a–c), persistent trigeminal artery (Fig. 2.16) and proatlantal intersegmental arteries [6].

Asymmetric caudal fusion of basilar artery is clinically important for any neurointerventionist, in cases of basilar tip aneurysms treatment, where the major network of perforators derives from the P1 segment which has the most cranial position (Fig. 2.17) [12].

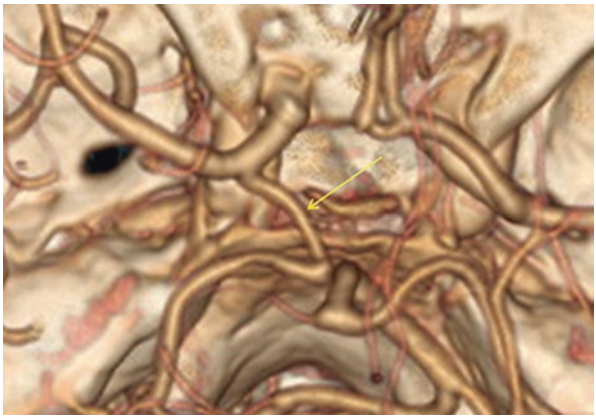

Fig. 2.11 CTA (VRT 3D reconstructions) shows a left sided Fetal Pcom (*yellow arrow*) (Reproduced from Zampakis et al. [6])

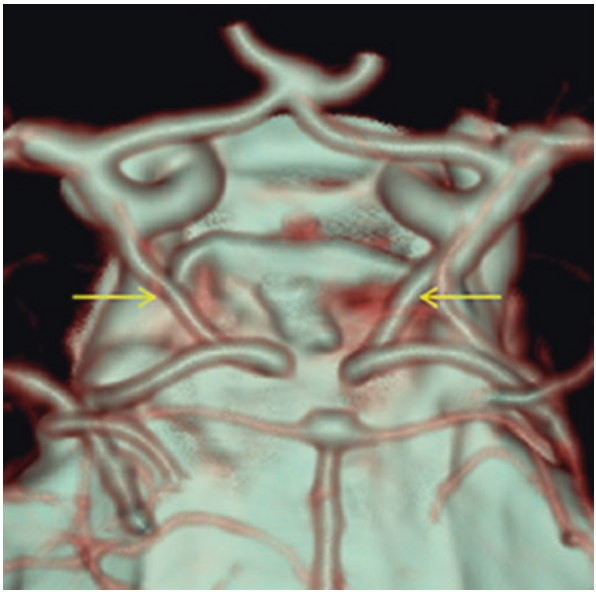

Fig. 2.12 CTA (VRT 3D reconstructions) shows bilateral Fetal Pcom (*yellow arrows*) (Reproduced from Zampakis et al. [6])

Anastomotic Pathways

Collateral supply to the brain comprises of three elements: The COW, leptomeningeal collaterals and extracranial–intracranial anastomoses.

COW plays an important role as a collateral supply in cases of acute or chronic cerebrovascular occlusive disease. It is best seen in CT or MR angiograms, ideally in 3D reconstructions. Anatomic variations of COW are the rule, since a complete COW is seen only in ~40 % of the people (Fig. 2.18) [13]. It is important to realize that COW collateral supply and morphologic changes, is a dynamic process that is influenced by several hemodynamic changes (Fig. 2.19).

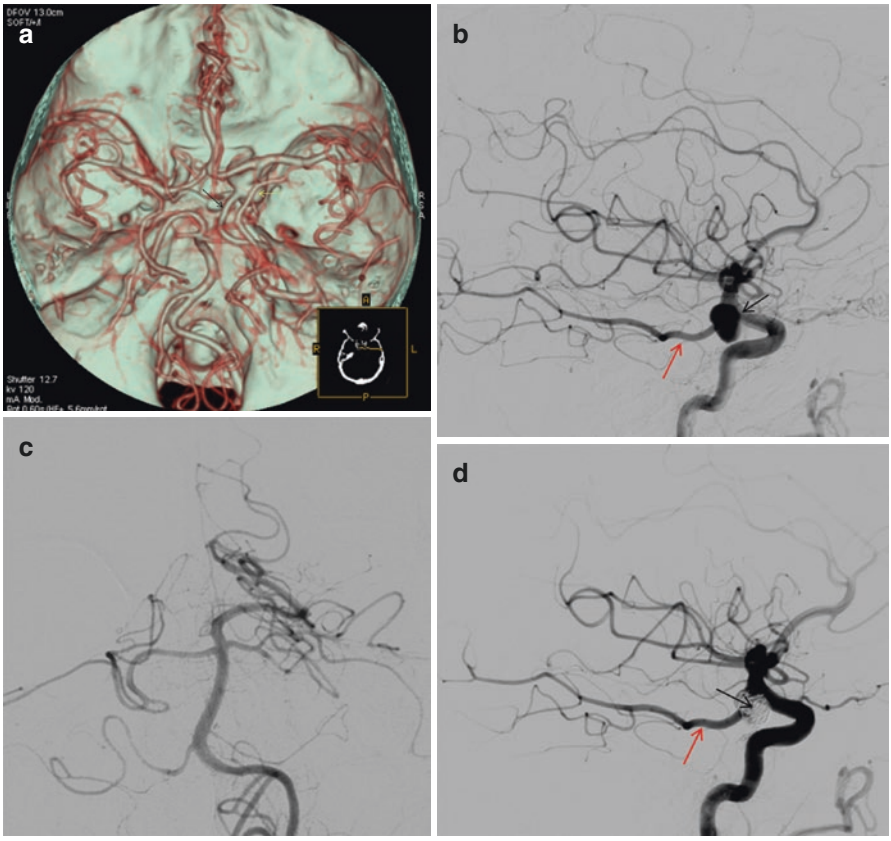

Fig. 2.13 (**a**) CTA (VRT reconstructions) shows a right sided Fetal Pcom (*black arrow*) with a large aneurysm at the origin of the vessel (*yellow arrow*) (Reproduced from Zampakis et al. [6]). (**b**) Digital substaction angiography (lateral view) of the right ICA, shows Fetal Pcom (*red arrow*) and large aneurysm at the origin of the vessel (*black arrow*), which cannot be compromised (Reproduced from Zampakis et al. [6]). (**c**) Digital substaction angiography (AP view) of the left vertebral artery. The posterior cerebral artery on the right is not opacified (definition of Fetal Pcom) (Reproduced from Zampakis et al. [6]). (**d**) Post-embolisation digital substaction angiography (lateral view) of the right ICA, shows good patency of Fetal Pcom (*red arrow*) and complete obliteration of the aneurismal sac (*black arrow*) (Reproduced from Zampakis et al. [6])

The extracranial—intracranial anastomoses are potential or actual anastomotic connections between branches of the external carotid artery and the internal carotid or vertebral arteries. They can play a role in chronic cerebrovascular occlusive disease (Fig. 2.20), but most importantly their knowledge is crucial for interventional endovascular procedures, in order to avoid hazardous complications, when injecting liquid material to ECA branches [14].

Finally, pial collaterals are end-to-end anastomoses between distal branches of the intracerebral arteries that potentially provide collateral flow across vascular watershed zones. These collateral networks play an important role in cases of stroke [15].

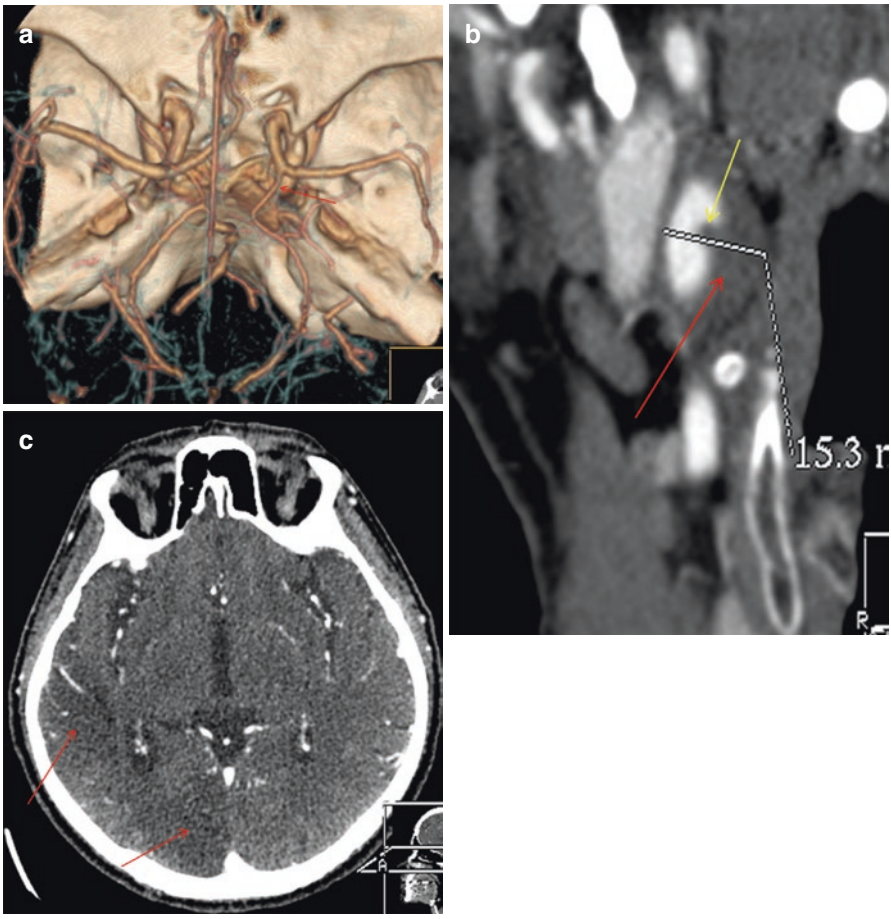

Fig. 2.14 (**a**) CTA (VRT reconstructions) shows a right sided Fetal Pcom (*red arrow*) (Reproduced from Zampakis et al. [6]). (**b**) CT oblique MPR image shows increased wall thickness (*red arrow*) and intimal flap (*yellow arrow*) of a dissected right ICA (Reproduced from Zampakis et al. [6]). (**c**) Axial CT image at the level of 3rd ventricle shows right sided occipital and posterior parietal lobe infarcts (*red arrows*) (Reproduced from Zampakis et al. [6])

Venous Cranial Anatomy and Variations

The cerebral venous system comprises of dural sinuses and cerebral veins and is divided into deep and superficial.

The main dural sinuses include the cavernous sinus, superior and inferior petrosal sinus, the superior sagittal sinus, the inferior sagittal sinus, the sphenoparietal sinus, the straight sinus, the transverse sinus and the sigmoid sinus.

Superficial cerebral veins collect the blood from the cortex and subcortical white matter. They join the superior sagittal sinus which along with the straight sinus

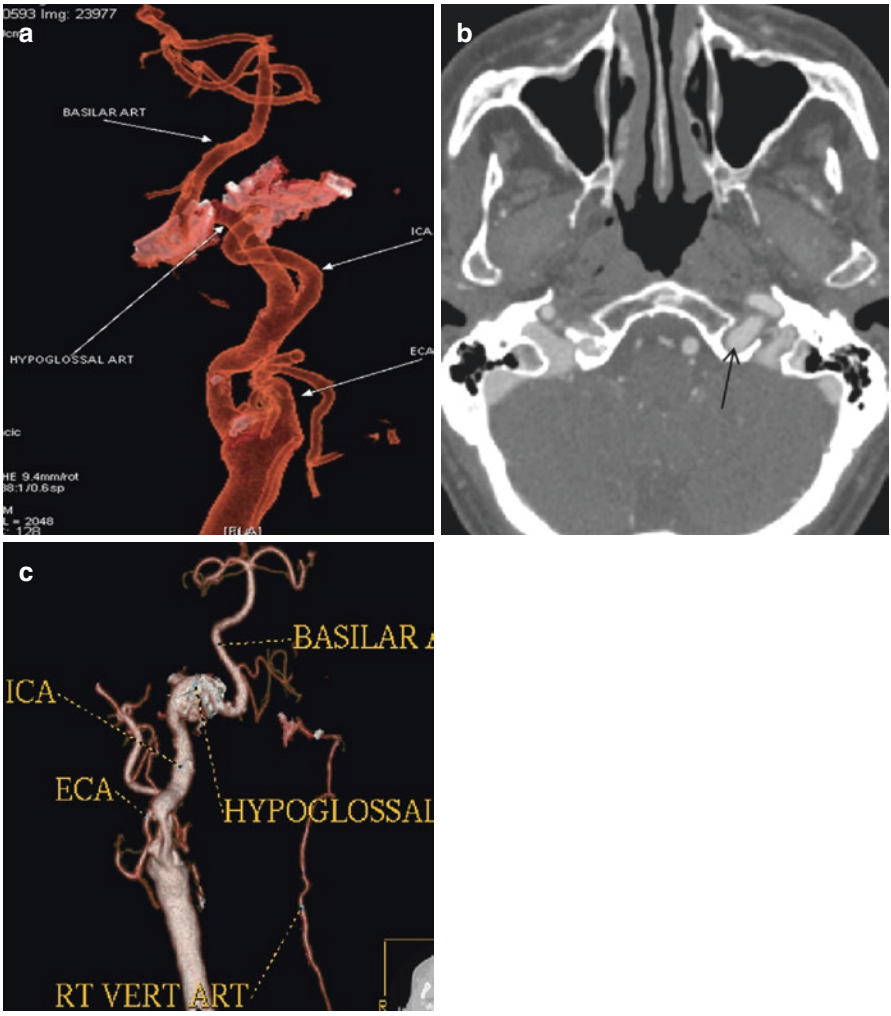

Fig. 2.15 (**a**) CTA (VRT 3D reconstructions) shows a vessel connecting the ICA with the basilar artery (annotations) (Reproduced from Zampakis et al. [6]). (**b**) Axial CT image at the level of hypoglossal canal shows an enlarged vessel piercing the skull base on the left, through the hypoglassal canal, which has been also enlarged (*black arrow*) (Reproduced from Zampakis et al. [6]). (**c**) CTA (VRT 3D reconstructions) reveals absent proximal vertebral artery and hypoplastic contralateral vertebral artery (annotations) (Reproduced from Zampakis et al. [6])

drains into the torcular herophili, where the lateral sinuses end up as well (Fig. 2.21a, b). Other major superficial cerebral veins include the anastomotic veins of Labbe and Trolard, as well as the middle cerebral veins.

The deep cerebral veins collect the blood from the deep white matter and basal ganglia. They consist of medullary and subependymal veins and the most important are the thalamostriate veins, the basal vein of Rosenthal and internal cerebral veins.

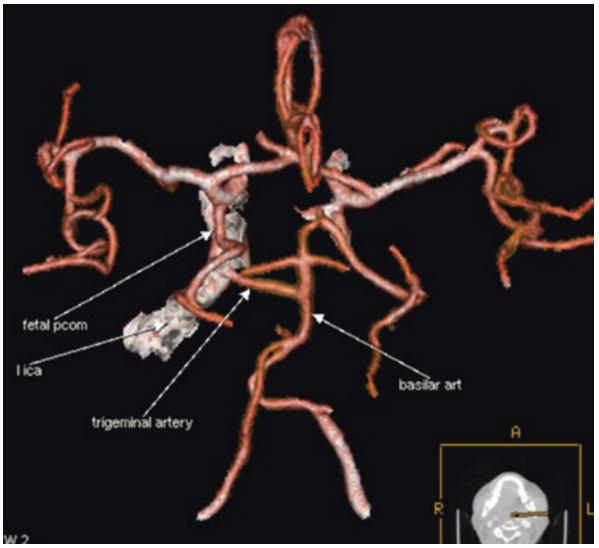

Fig. 2.16 CTA (VRT 3D reconstructions) shows a left-sided trigeminal artery joining the basilar artery. The basilar artery (which is relatively hypoplastic, proximal to the connection site) gives rise to the right PCA while the left PCA arises from the ICA (fetal PCom) (Saltzman's type II or Weon's type 3) (annotations) (Reproduced from Zampakis et al. [6])

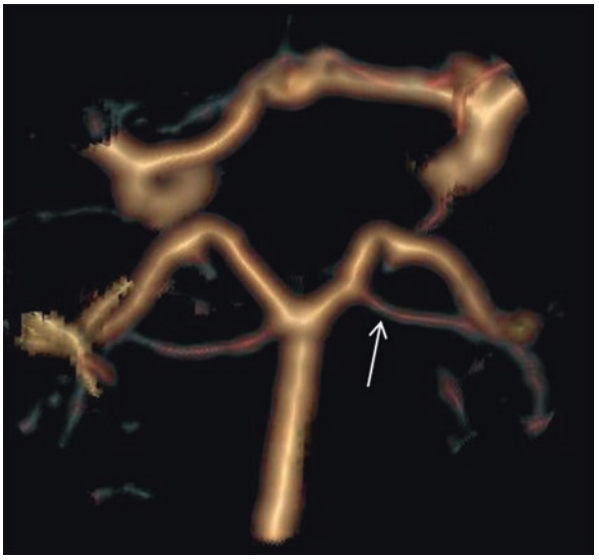

Fig. 2.17 CTA (VRT 3D reconstruction) shows a right-sided asymmetrical caudal fusion of the basilar artery. *White arrow* indicates the origin of the R SCA from the ipsilateral P1 segment of PCA

Fig. 2.19 (**a**) 3 T MRA in a 10y old girl with a vertebrovertebral fistula (VVF) on the right side (*black circle*). Note the enlargement of both posterior communicating arteries (*white arrows*) as part of the COW reconstitution due to the arterial steal from the fistula. (**b**) Axial CT image at the level of carotid canals shows a hypoplastic right ICA, along with the hypoplastic ipsilateral carotid canal (*white arrow*). (**c**) CTA of the brain (MIP reconstruction-Superior view). Note the enlargement of right posterior communicating artery (*white arrow*) as part of the COW reconstitution due to the ipsilateral carotid hypoplasia

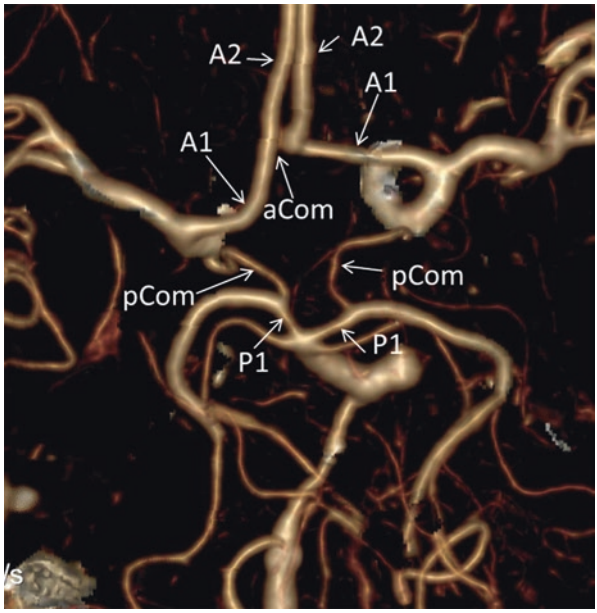

Fig. 2.18 CTA (VRT 3D reconstruction) A complete COW is seen. All parts of COW are annotated

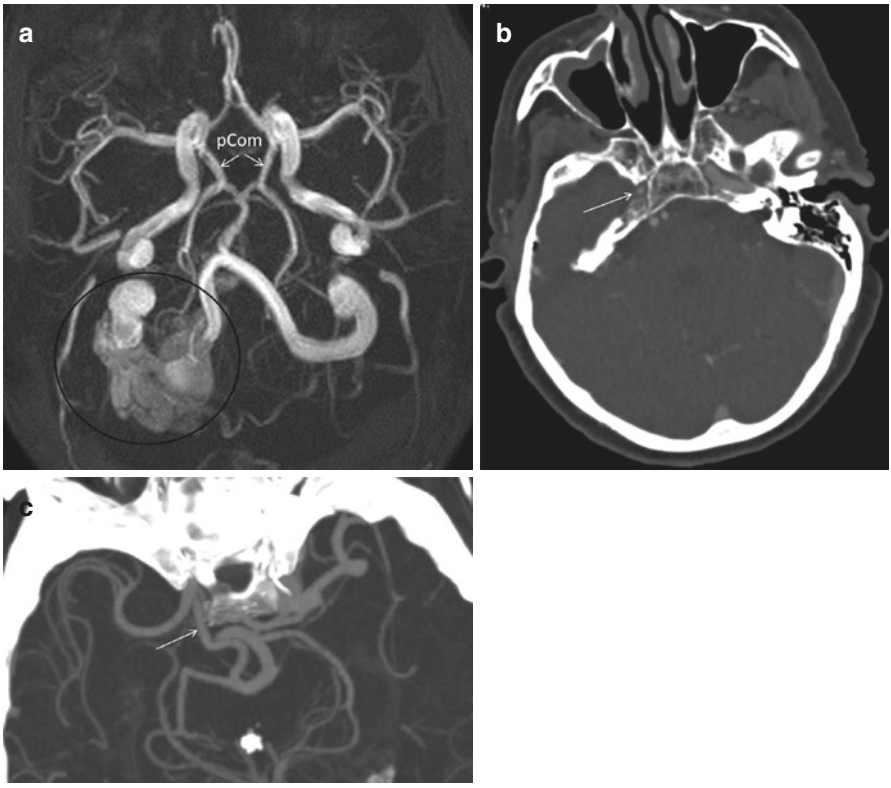

Fig. 2.20 CTA (VRT 3D reconstruction) *Blue short arrows* indicate the profound VA-ECA anastomosis between temporal artery and vertebral artery, due to total occlusion of the ipsilateral common carotid artery

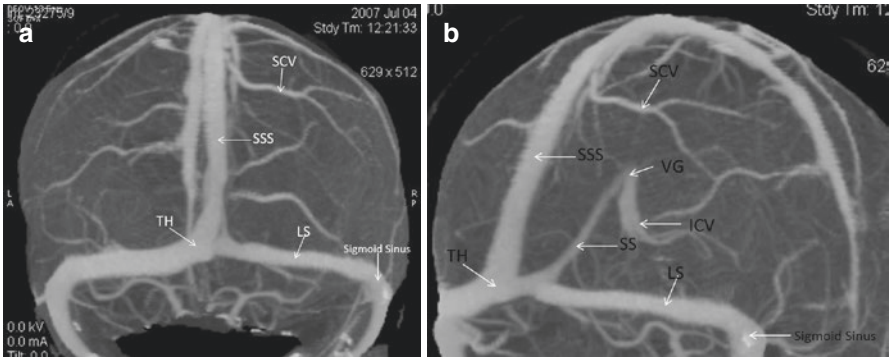

Fig. 2.21 (**a**) CT Venography of the brain (MIP reconstructions-AP View). *White arrows* indicate main venous sinuses and veins. *SSS* superior sagittal sinus, *SCV* superior cerebral vein, *LS* lateral sinus, *TH* torcular herophili, (**b**) CT Venography of the brain (MIP reconstructions-Oblique View). *White arrows* indicate main venous sinuses and veins. *SSS* superior sagittal sinus, *SS* straight sinus, *SCV* superior cerebral vein, *LS* lateral sinus, *TH* torcular herophili, *VG* vein of galen

The confluence of internal cerebral and basal veins of Rosenthal gives rise to the midline great vein of Galen, which enters the straight sinus (Fig. 2.21a, b).

The superior petrosal sinuses connect the cavernous sinus to the sigmoid sinuses, while the inferior petrosal sinuses connect the cavernous sinus to the jugular vein.

The deep sub-ependymal veins are rather constant, while the superficial cortical veins are extremely variable.

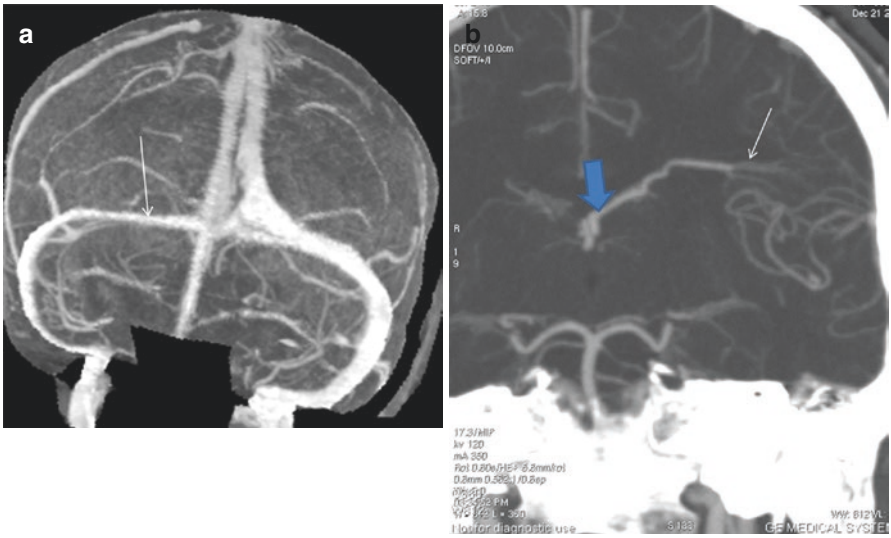

Fig. 2.22 (**a**) CT Venography of the brain (MIP reconstructions-AP View). *White arrow* indicates the hypoplastic left lateral sinus. (**b**) CT Venography of the brain (coronal MPR reconstruction) shows a left-sided developmental venous anomaly (DVA). *White arrow* indicates the characteristic "medusa-head" appearance of the DVA, while the *thick blue arrow* shows the deep venous drainage into the unilateral internal cerebral vein

Finally, the anatomy of the posterior fossa veins is quite variable, but the main drainage pathways include a superior (Galenic), an inferior (petrosal) and a posterior (tentorial) group of veins.

Although true anomalies of the deep and superficial venous system are quite rare, anatomic variations are not. The most common include asymmetric transverse sinuses (the left being more often hypoplastic than the right, due to pulsations of the right atrium and larger capacity of the right jugular system) and developmental venous anomalies (DVAs) (Fig. 2.22a, b).

References

1. Lasjaunias P, Berenstein A, ter Brugge K. Surgical neuroangiography, Clinical vascular anatomy and variations, vol. 1. 2nd ed. Berlin: Springer; 2001.
2. Bouthillier A, van Loveren HR, Keller JT. Segments of the internal carotid artery: a new classification. Neurosurgery. 1996;38(3):425–32.
3. Paulsen F, Tillman B, Christofides C, Richter W, Koebke J. Curving and looping of the internal carotid artery in relation to the pharynx: frequency, embryology and clinical implications. J Anat. 2000;197:373–81.
4. Wasserman JM, Sclafani SJ, Goldstein NA. Intraoperative evaluation of a pulsatile oropharyngeal mass during adenotonsillectomy. Int J Pediatr Otorhinolaryngol. 2006;70:371–5.
5. Kay DJ, Mehta V, Goldsmith AJ. Perioperative adenotonsillectomy management in children: current practices. Laryngoscope. 2003;113:592–7.

6. Zampakis P, Panagiotopoulos V, Petsas T, Kalogeropoulou C. Common and uncommon intracranial arterial anatomic variations in multi-detector computed tomography angiography (MDCTA). What radiologists should be aware of. Insights Imaging. 2015;6(1):33–42.
7. Lasjaunias P, Berenstein A, ter Brugge K. Surgical neuroangiography, Clinical vascular anatomy and variations, vol. 1. 2nd ed. Berlin: Springer; 2001. p. 602–5.
8. Chang HY, Kim MS. Middle cerebral artery duplication: classification and clinical implications. J Korean Neurosurg Soc. 2011;49(2):102–6.
9. Lasjaunias P, Berenstein A, ter Brugge K. Surgical neuroangiography, Clinical vascular anatomy and variations, vol. 1. 2nd ed. Berlin: Springer; 2001. p. 593–6.
10. Lin WC, Hsu SW, Kuo YL, Feekes JA, Wang HC. Combination of olfactory course anterior cerebral artery and accessory middle cerebral artery (MCA) with occluded in situ MCA and related moyamoya phenomenon. Brain Dev. 2009;31(4):318–21.
11. Komiyama M, Yasui T. Accessory middle cerebral artery and moyamoya disease. J Neurol Neurosurg Psychiatry. 2001;71:129–30.
12. Lasjaunias P, Berenstein A, ter Brugge K. Surgical neuroangiography, Clinical vascular anatomy and variations, vol. 1. 2nd ed. Berlin: Springer; 2001. p. 536.
13. Kapoor K, Singh B, Dewan LIJ. Variations in the configuration of the circle of Willis. Anat Sci Int. 2008;83(2):96–106.
14. Lasjaunias P, Berenstein A, ter Brugge K. Surgical neuroangiography, Clinical vascular anatomy and variations, vol. 1. 2nd ed. Berlin: Springer; 2001. p. 188.
15. Bhattacharya JJ, Forbes K, Zampakis P, Bowden DJ, Stevens JM. Overview of anatomy, pathology and techniques. In: Adam A, Dixon A, Gillard J, Schaefer-Prokop CM, editors. Grainger and Allison's diagnostic radiology. A textbook of medical imaging, vol. 2. 6th ed. Churchill Livingstone: Elsevier; 2014. p. 1418. Chapter 60.